Human Epithelial Cystic Fibrosis Transmembrane Conductance Regulator without Exon 5 Maintains Partial Chloride Channel Function in Intracellular Membranes

Junxia Xie,* Mitchell L. Drumm,# Jiying Zhao,* Jianjie Ma,* and Pamela B. Davis*#
Departments of *Physiology and Biophysics and #Pediatrics, Case Western Reserve University School of Medicine, Cleveland, Ohio 44106 USA

ABSTRACT The cardiac isoform of the cystic fibrosis transmembrane conductance regulator (CFTR) is a splice variant of the epithelial CFTR, which lacks 30 amino acids encoded by exon 5 in the first intracellular loop. For examination of the role of exon 5 in CFTR channel function, a CFTR deletion mutant, in which exon 5 was removed from the human epithelial CFTR, was constructed. The wild type and Δexon5 CFTR were expressed in a human embryonic kidney cell line (293 HEK). Fully mature glycosylated CFTR (~170 kDa) was immunoprecipitated from cells transfected with wild type CFTR cDNA, whereas cells transfected with Δexon5 CFTR express only a core-glycosylated form (~140 kDa). The Western blot test performed on subcellular membrane fractions showed that Δexon5 CFTR was located in the intracellular membranes. Neither incubation at lower temperature (26°C) nor stimulation of 293 HEK cells with forskolin or CPT-cAMP caused improvement in glycosylation and processing of Δexon5 CFTR proteins, indicating that the human epithelial CFTR lacking exon 5 did not process properly in 293 HEK cells. On incorporation of intracellular membrane vesicles containing the Δexon5 CFTR proteins into the lipid bilayer membrane, functional phosphorylation- and ATP-dependent chloride channels were identified. CFTR channels with an 8-pS full-conductance state were observed in 14% of the experiments. The channel had an average open probability (P_o) of 0.098 ± 0.022, significantly less than that of the wild type CFTR (P_o = 0.318 ± 0.028). More frequently, the Δexon5 CFTR formed chloride channels with lower conductance states of ~2-3 and ~4-6 pS. These subconductance states were also observed with wild type CFTR but to a much lesser extent. Average P_o for the 2–3-pS subconductance state, estimated from the area under the curve on an amplitude histogram, was 0.461 ± 0.194 for Δexon5 CFTR and 0.332 ± 0.142 for wild type (p = 0.073). The data obtained indicate that deleting 30 amino acids from the first intracellular loop of CFTR affects both processing and function of the CFTR chloride channel.

INTRODUCTION

The cystic fibrosis transmembrane conductance regulator (CFTR) consists of five major domains, with two membrane-spanning domains, two nucleotide binding domains (NBDs), and a regulatory (R) domain (Riordan et al., 1989). The CFTR forms a chloride channel of linear conductance (Anderson et al., 1991a; Bear et al., 1992), which is regulated by cAMP-dependent protein kinase phosphorylation (Anderson et al., 1991b; Cheng et al., 1991; Rich et al., 1993; Chang et al., 1993) at multiple sites in the R domain and binding and hydrolysis of ATP by the NBDs (Anderson et al., 1991b; Quinton and Reddy, 1992; Nagel et al., 1992; Baukrowitz et al., 1994).

The membrane-spanning domains of the CFTR are joined by six extracellular and four intracellular loops of different peptide sequences, the functions of which are largely unknown. Our previous research showed that the second intracellular loop joining transmembrane segments IV and V of CFTR played an important role in the function of the CFTR. Deleting 19 amino acids from this loop caused retention of the CFTR in the intracellular membranes and also altered the distribution of subconductance states of the CFTR channel (Xie et al., 1995).

The first intracellular loop (amino acid 139–194) connects transmembrane segments II and III, and 30 of the residues in this loop (TLKLSSRVLDKISIGQLVSLLSNNLNKFDE, amino acid 164–193) are encoded by exon 5. To investigate the role of the first intracellular loop in CFTR function, we constructed a CFTR deletion mutant (Δexon5 CFTR), in which 30 amino acids were removed from the first intracellular loop. This region was chosen because Δexon5 CFTR is an alternatively spliced CFTR isoform expressed predominantly in heart membranes of some species (Horowitz et al., 1993). Previous studies with rabbit and guinea pig ventricular myocytes identified a protein kinase A- (PKA-) regulated chloride channel with conduction properties similar to those of the epithelial CFTR, which has been assumed to be attributable to Δexon5 CFTR (Nagel et al., 1992; Levesque et al., 1992), and the rabbit Δexon5 CFTR gives typical cAMP-regulated chloride conductance in *Xenopus* oocytes (Hart et al., 1996). However, when human epithelial CFTR lacking exon 5 is expressed in HeLa cells, it fails to generate cAMP-mediated chloride transport because of apparent defective intracellular processing (Delaney et al., 1993). Consequently, the single-channel properties of Δexon5 CFTR in intracellular membranes have not been studied.

Received for publication 24 June 1996 and in final form 30 August 1996.
Address reprint requests to Dr. Pamela B. Davis, Deparment of Physiology, Biophysics and Pediatrics, Case Western University School of Medicine, Cleveland, OH 44106. Tel.: 216-368-4370; Fax: 216-368-4223; E-mail: pbd@po.cwru.edu.

0006-3495/96/12/3148/09 $2.00

In this study, human Δexon5 and wild type CFTR cDNA were expressed in 293 HEK cells. Consistent with the study of Delaney et al. (1993), we found that Δexon5 is a processing mutant, with the mutant CFTR proteins retained primarily in the intracellular membranes. On reconstitution of intracellular membrane vesicles containing Δexon5 CFTR into planar lipid bilayer, we found that Δexon5 CFTR formed functional chloride channels, which open primarily to the subconductance states.

MATERIALS AND METHODS

Subcloning of the CFTR gene

The Δexon5 CFTR gene, which lacks 90 nucleotides (622 to 712), was cloned into the EcoRI site of pBluescript. After confirmation of the deletion mutation by sequence analysis, the mutant gene was shuttled into the pCEP4 vector between PvuII and AflII enzyme restriction sites by substitution of the corresponding fragment in pCEP4 wild type (WT; Drumm et al., 1991) with the mutated fragment between SmaI and AflII enzyme restriction sites. The identity of the mutant clone, pCEP4(Δexon5), was confirmed by restriction enzyme digestions.

Cell culture

A human embryonic kidney cell line (293-EBNA, Invitrogen, San Diego, CA) was used for transfection and expression of WT and mutant CFTR proteins. The culture conditions for maintaining the 293 HEK cells were as decribed previously (Xie et al., 1995). Because of rapid downregulation of Δexon5 CFTR protein expressed during the stable selection process, transient transfection with lipofectAMINE reagent (Life Technologies, Inc., Gaithersburg, MD) was used for the CFTR gene expression in this study. The parent cell line was grown to confluence in a 37°C incubator with 5% CO_2 and passaged 1:5 2 days before the gene transfer. We then introduced plasmid pCEP4(WT), pCEP4(ΔF508) (Drumm et al., 1991), pCEP4(Δ19) (Xie et al., 1995), or pCEP4(Δexon5) into 293 HEK cells, using lipofectAMINE reagent (Hawley-Nelson et al., 1993). Two days after transfection, the cells were used for immunoprecipitation/Western blot assay, isolation of membrane vesicles on a discontinuous sucrose density gradient, and reconstitution studies in the lipid bilayer membranes.

Immunoprecipitation/Western blot assay of CFTR

293 HEK cells freshly transfected with pCEP4(WT), pCEP4(ΔF508), pCEP4(Δ19), or pCEP4(Δexon5) were cultured for 2 days. The procedures are essentially the same as described previously (Xie et al., 1995), except that monoclonal antibody (mouse antihuman, 2 μg) which is specific for the C-terminus of CFTR (mAb 24–1; Genzyme, Cambridge, MA) was used for the immunoprecipitation and subsequent immunoblotting assay. Cell lysis supernatant (48,000 × g, 1 h, 4°C) containing 30 mg total protein, was immunoprecipitated for each sample. The precipitated protein was solubilized with 30 μl gel sample buffer (200 mM Tris-Cl pH 6.7, 9% SDS, 6% β-mercaptoethanol, 15% glycerol, 0.01% bromphenol blue) and loaded onto a 5% SDS-polyacrylamide gel. The proteins were then transferred to a PVDF membrane (Bio-Rad, Hercules, CA) and probed with monoclonal antibody (mAb 24–1, 0.8 μg/ml). A secondary peroxidase-conjugated affinity purified goat antibody to mouse IgG (Organon Teknika Corp., West Chester, PA) was added to allow visualization of the CFTR-antibody complex. The proteins were detected by chemiluminescence according to the manufacturer's recommendation (SuperSignal CL-HRP substrate system; Pierce, Rockford, IL).

Subcellular fractionation of membrane vesicles

Six to twelve 75-cm^2 flasks of 293 HEK cells transfected with pCEP4 (WT), pCEP4 (ΔF508), or pCEP4 (Δexon5) vectors were harvested by scraping from the flask bottom following three washes with ice-cold phosphate-buffered saline (137 mM NaCl, 10 mM Na_2HPO_4, 2.7 mM KCl, 5 μM diisopropyl fluorophosphate, 1.8 mM KH_2PO_4, pH 7.4). The cells were disrupted with a combination of hypotonic lysis and Dounce homogenization (Xie et al., 1995) in the presence of protease inhibitors (5 μM diisopropyl fluorophosphate, 10 μg/ml pepstatin A, 10 μg/ml aprotinin, and 9.6 mg/ml benzamidine). Microsomes were isolated by sequential centrifugation at 6,000 × g for 20 min at 4°C and at 100,000 × g for 45 min at 4°C. The microsomes were resuspended in either 600 μl isotonic buffer (250 mM sucrose, 1 mM EDTA, 10 mM Hepes; pH 7.2) or prephosphorylation buffer (250 mM sucrose, 10 mM Hepes pH 7.2, 5 mM ATP, 5 mM $MgCl_2$, and 100 units/ml PKA catalytic subunit). Further separation of plasma and intracellular membranes was carried out on a discontinuous sucrose density gradient (10,000 × g, 6 h, 4°C) with a swinging bucket rotor (SW28). The composition of the sucrose density gradient is 28.0%, 33.0%, 36.0%, 38.7%, 43.7%, (see Fig. 2 *A*). After centrifugation, the membrane fractions were collected from the interfaces, washed, and resuspended in isotonic buffer of 250 mM sucrose, 1 mM EDTA, 10 mM Hepes; pH 7.2. Proteins (100 μg) from each fraction were denatured with 6× gel sample buffer (300 mM Tris-Cl pH 6.8, 600 mM dithiothreitol, 12% SDS, 0.6% bromphenol blue) and loaded onto a 5% SDS-polyacrylamide gel. The proteins were then transferred to PVDF membrane (Bio-Rad) and detected as described for the immunoprecipitation/Western blot assay.

Reconstitution of the CFTR chloride channel

Lipid bilayer membranes were formed across an aperture of ~200-μm diameter with a lipid mixture of phosphatidylethanolamine:phosphatidylserine:cholesterol in a ratio of 6:6:1; the lipids were dissolved in decane at a concentration of 40 mg/ml (Xie et al., 1995; Tao et al., 1996; Ma et al., 1996). The recording solutions contained *cis* (intracellular): 200 mM KCl, 2 mM ATP-Mg, and 10 mM Hepes-Tris (pH 7.4); *trans* (extracellular): 50 mM KCl and 10 mM Hepes-Tris (pH 7.4). Membrane vesicles (1–3 μl) containing WT or Δexon5 proteins were added to the *cis* solution (1 ml total volume). 50 units/ml of PKA catalytic subunit (Promega, Madison, WI) were always present in the *cis* solution. Single-channel currents were recorded with an Axopatch 200A patch-clamp unit (Axon Instrument, Foster City, CA). Data acquisition and pulse generation were performed with a 486 computer and 1200 Digidata analog-to-digital–digital-to-analog converter (Axon Instrument). The analyses of single-channel data were performed with pClamp software (Axon Instrument) and custom programs. Data presented in this paper were obtained from six different preparations of membrane vesicles isolated from 293 HEK cells transfected with Δexon5 CFTR.

RESULTS

ΔExon5 CFTR is a temperature-insensitive processing mutant in 293 HEK cells

The CFTR gene was introduced into 293 HEK cell as described in Materials and Methods. To confirm CFTR expression, we performed immunoprecipitation/Western blot assays on the transfected cells. Cells transfected with pCEP4(WT) expressed fully glycosylated CFTR protein with a molecular mass of ~170 kDa, plus some core glycosylated CFTR proteins (~140 kDa; Fig. 1). Cells transfected with pCEP4(ΔF508), pCEP4(Δ19), or pCEP4(Δexon5) expressed only the core-glycosylated form of CFTR, with a molecular mass of ~140 kDa (Fig. 1). Two

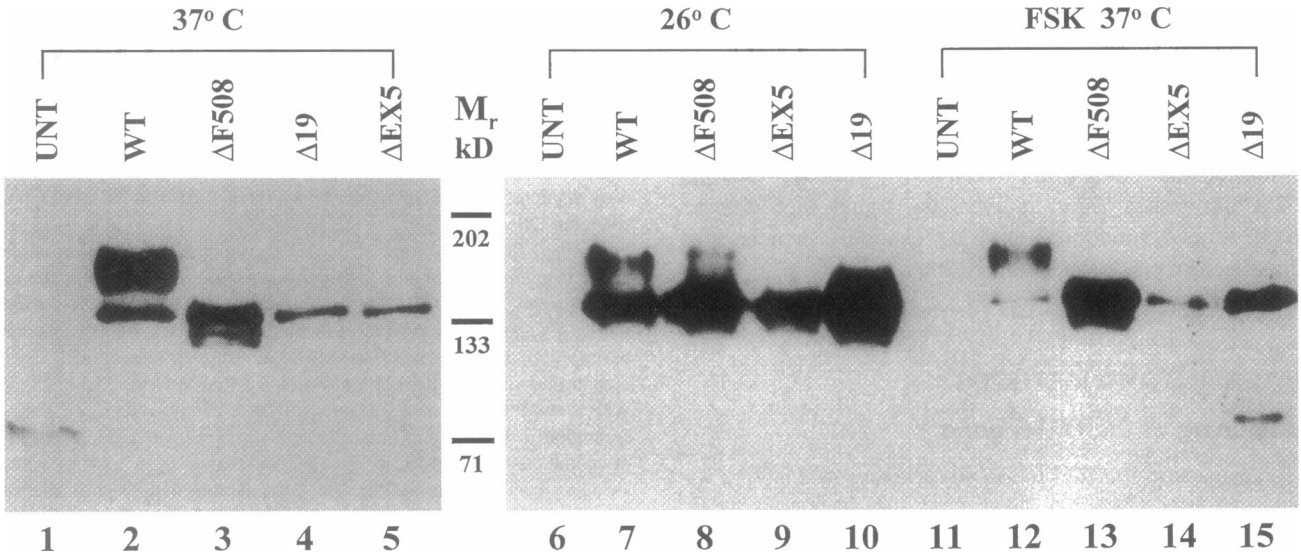

FIGURE 1 Immunoprecipitation and Western blot assay of CFTR. Lysates of 293 HEK cells transfected with pCEP4 (WT), pCEP4 (ΔF508), pCEP4 (Δ19), or pCEP4 (Δexon5) were immunoprecipitated and blotted as described in Methods and Materials. 30 mg of total cell lysate protein was precipitated and loaded on each lane, except for 15 mg on lane 2. The proteins were visualized by exposure of the blot to a Kodak X-Omat antireflection film for 2 min. Lanes 1, 6, and 11 (*UNT*): untransfected 293 HEK cells. Lanes 2, 7, and 12 (*WT*): WT CFTR expressing cells. Lanes 3, 8, and 13 (*ΔF508*): ΔF508 CFTR expressing cells. Lanes 4, 10, and 15 (*Δ19*): Δ19 CFTR expressing cells. Lanes 5, 9, and 14 (*Δex5*): Δexon5 CFTR expressing cells. Lanes labeled 26°C were cells cultured for 2 days at 37°C after transfection followed by incubation at 26°C for 48 h before the experiment. Lanes labeled 37°C were cells cultured for 2 days at 37°C after transfection before experiment. Lanes labled FSK 37°C were cells cultured for 2 days at 37°C after transfection followed by incubation in serum-free media containing 1% glutamine and 20 μM forskolin at 37°C for 48 h before the experiment.

protein bands with molecular mass <140 kDa were also clearly present for ΔF508 CFTR expressing cells (Fig. 1), which are probably due to the alternative translation initiation sites within the CFTR protein (Pind et al., 1995). These lower bands were also present in the WT, Δ19, and Δexon5 CFTR expressing cells (Figs. 1 and 2).

It was shown previously that the processing of ΔF508 CFTR is temperature sensitive (Denning et al., 1992; Lukacs et al., 1993). As shown in Fig. 1, ΔF508 CFTR, which appeared only in the core-glycosylated form at 37°C, appeared in the fully glycosylated form when the culture temperature was lowered to 26°C (Fig. 1, lane 8). However, incubation of either pCEP4 (Δexon5) or pCEP4 (Δ19) transfected cells at 26°C for 48 h did not increase the amount of CFTR protein in the fully glycosylated form (Fig. 1, lanes 9 and 10; see also Xie et al., 1995). Thus, Δexon5 CFTR appears to be a temperature-insensitive processing mutant in 293 HEK cells.

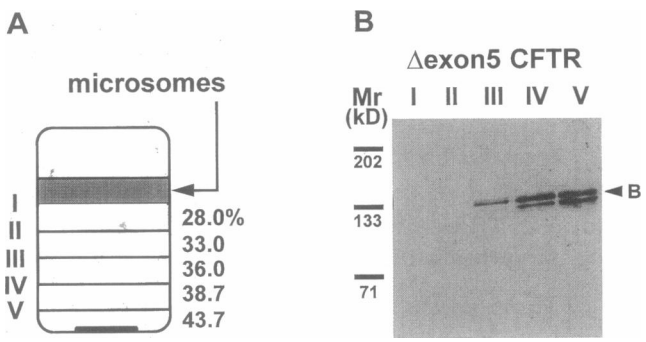

FIGURE 2 Subcellular fractionation and Western blot assay of Δexon5 CFTR. (*A*) Illustration of discontinuous sucrose gradient to separate plasma membrane from intracellular membranes for cells transfected with Δexon5 CFTR. (*B*) 100 μg of total protein from each fraction was subjected to 5% SDS-polyacrylamide gel electrophoresis. Fractions were (*I*) top of the gradient, (*II*) 28%/33% interface, (*III*) 33%/36% interface, (*IV*) 36%/38.7% interface, and (*V*) 38.7%/43.7% interface. CFTR protein was detected as described in Materials and Methods. (←*B*) Core-glycosylated Δexon5 CFTR protein.

In rabbit and guinea pig heart, only CFTR message that lacks exon 5 is detected (Horowitz et al., 1993), yet cAMP regulated chloride channel, which is characteristic of CFTR, is observed in the plasma membrane patch (Nagel et al., 1992; Levesque et al., 1992). One difference between cardiac and epithelial cells is that the cardiac cells are constantly exposed to β-adrenergic stimulation. To test whether the human epithelial Δexon5 CFTR could process to the cell surface membrane on PKA phosphorylation, we performed immunoprecipitation/Western blot assay with cells preincubated in media containing either forskolin or 8-(4-chlorophenylthio)-cAMP for 2 days. Fig. 1 shows that 20 μM forskolin (n = 3) did not increase the amount of Δexon5 CFTR in its fully glycosylated form, nor did the 8-(4-chlorophenylthio)-cAMP (4 mM, n = 1; data not shown). Thus, phosphorylation of the CFTR protein did not cause improvement in the processing of the Δexon5 CFTR in 293 HEK cells.

ΔExon5 CFTR proteins are retained in the intracellular membranes

To characterize the subcellular localization of the Δexon5 CFTR protein, we fractionated the microsomal membrane vesicles, using a discontinuous sucrose density gradient (Fig. 2 *A*). Using this procedure, we showed previously that the fully glycosylated CFTR proteins were localized predominantly in fractions II and III (plasma membranes) and that the core-glycosylated CFTR proteins resided mainly in fractions IV and V (intracellular membranes) (Xie et al., 1995). Fig. 2 *B* shows that the Δexon5 CFTR protein was present mainly in fractions IV and V, with a molecular mass of approximately 140 kD. This intracellular localization of Δexon5 CFTR further indicates that deletion of exon 5 causes misprocessing of CFTR protein.

ΔExon5 CFTR forms a functional chloride channel with reduced open probability

To study the function of Δexon5 CFTR, we incorporated intracellular membrane vesicles (fractions IV and V from the sucrose density gradient) that contained Δexon5 CFTR into lipid bilayer membranes. This function was compared with that of the WT CFTR obtained from plasma membrane vesicles. The WT CFTR formed a PKA phosphorylation-dependent chloride channel with linear conductance of 8.2 ± 0.6 pS in 200 mM KCl; an average open probability (P_o) of 0.318 ± 0.028 was measured at −80 mV with 2 mM ATP present in the *cis*-intracellular solution (Xie et al., 1995).

When intracellular membrane vesicles containing Δexon5 CFTR were incorporated into the lipid bilayer membrane, functional chloride channels were observed. The single-channel currents shown in Fig. 3 *B* were representative of the 8-pS full conductance state (H state) of the Δexon5 CFTR channel. This 8-pS chloride channel was observed in 11 of 81 of the experiments, in which functional chloride channels were incorporated into the bilayer membrane (Fig. 3 and Table 1). This channel is characteristic of CFTR, as its opening absolutely requires the presence of PKA and ATP in the *cis* solution, and its activity could be completely blocked by 3 mM DPC added to the *trans* solution (data not shown). An average open probability measured with the 50% threshold criteria is 0.098 ± 0.022 for the Δexon5 CFTR channel at −80 mV. This value is significantly lower than that for the WT CFTR channel (P_o = 0.318 ± 0.028) measured by the same method.

Both WT and Δexon5 CFTR had slow kinetics of gating, with mean open lifetimes of τ_{o1} = ~10-20 ms (fast gating) and τ_{o2} = ~100-120 ms (slow gating). The cumulative open-time histogram in Fig. 4 shows that the distribution of fast and slow open events is significantly different for the Δexon5 and the WT CFTR channels. First, the total number of events was less for the Δexon5 channel than for the WT channel within the same recording period (compare the plateau phases of Fig. 4 *A* and *B*). Second, the relative

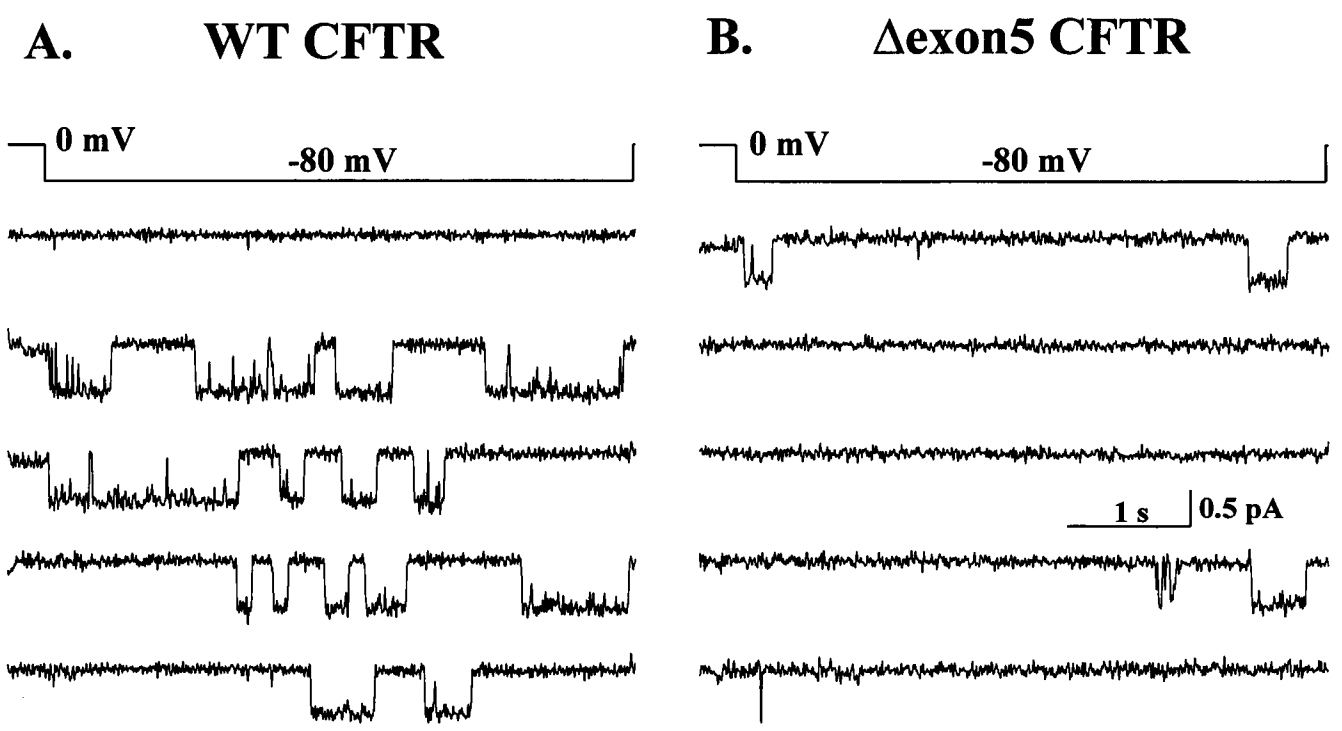

FIGURE 3 Reconstitution of WT and Δexon5 CFTR chloride channel in lipid bilayer membranes. Represented are consecutive single-channel current traces at −80 mV from a WT CFTR (*A*) and a Δexon5 CFTR channel (*B*). Here, both channels opened to the full conductance state (H state). The current amplitude for WT was −0.66 pA and for Δexon5 was −0.65 pA.

TABLE 1 Occurrence comparison of conductance states between WT and Δexon5 CFTR channels

Conductance state	WT CFTR*	Δexon5 CFTR
L (2–3 pS)	26 (17%)	67 (82.7%)
M (4–6 pS)	2 (1.3%)	3 (3.7%)
H (~8 pS)	124 (81.5%)	11 (13.6%)
Number of experiments	152	81

These experiments were performed with 2 mM ATP-Mg present in the *cis*-intracellular solution and 0 mM $MgCl_2$ present in the *trans*-extracellular solution. The current carriers were 200 mM (*cis*)/50 mM (*trans*) KCl. *Data from Tao et al. (1996).

occurrence of the long open events (τ_{o2}) was significantly less frequent for the Δexon5 (W_{o2}/W_{o1} = 1.73) channel than for the WT (W_{o2}/W_{o1} = 7.67) CFTR channel (Fig. 4). This altered distribution of the open-lifetime histogram, together with the reduced number of open events, probably accounts for the reduced activity of the Δexon5 CFTR channel (Fig. 3 *B*).

ΔExon5 CFTR formed chloride channels with subconductance states

In systematic studies we found that Δexon5 CFTR tends to form chloride channels with lower conductance states (Fig. 5). Most frequently, we would observe a 2–3-pS conductance chloride channel with the intracellular membrane vesicles containing the Δexon5 CFTR proteins (Fig. 5 *A*). On a few occasions we could identify an intermediate conductance state of 4–6 pS (Fig. 5 *B*). The following data suggest that these open events were generated by the Δexon5 CFTR protein. First, opening of these channels absolutely required the presence of ATP and PKA in the *cis*-intracellular solution; without PKA or ATP no such open events were recorded in more than 30 bilayer fusions with vesicles containing Δexon5 CFTR. Second, none of these events was ever seen with vesicles from untransfected 293 HEK cells with ($n > 20$) or without ($n > 30$) PKA and ATP. Third, under a concentration gradient of 200 mM KCl (*cis*)/50 mM KCl (*trans*) these channels exhibited approximately linear current–voltage relationships with reversal potentials that were close to the Nernst potential for chloride (Fig. 5 *C*), indicating that the channels were selective for chloride ions. Finally, these low-conductance chloride channels were sensitive to blockade by DPC but not by DIDS (Fig. 6). All these properties are characteristic of the CFTR chloride channel.

We showed previously that the WT CFTR channel contains two distinct subconductance states of 5–6 pS (M) and 2.7 pS (L), in addition to the full conductance state (H; 8 pS)

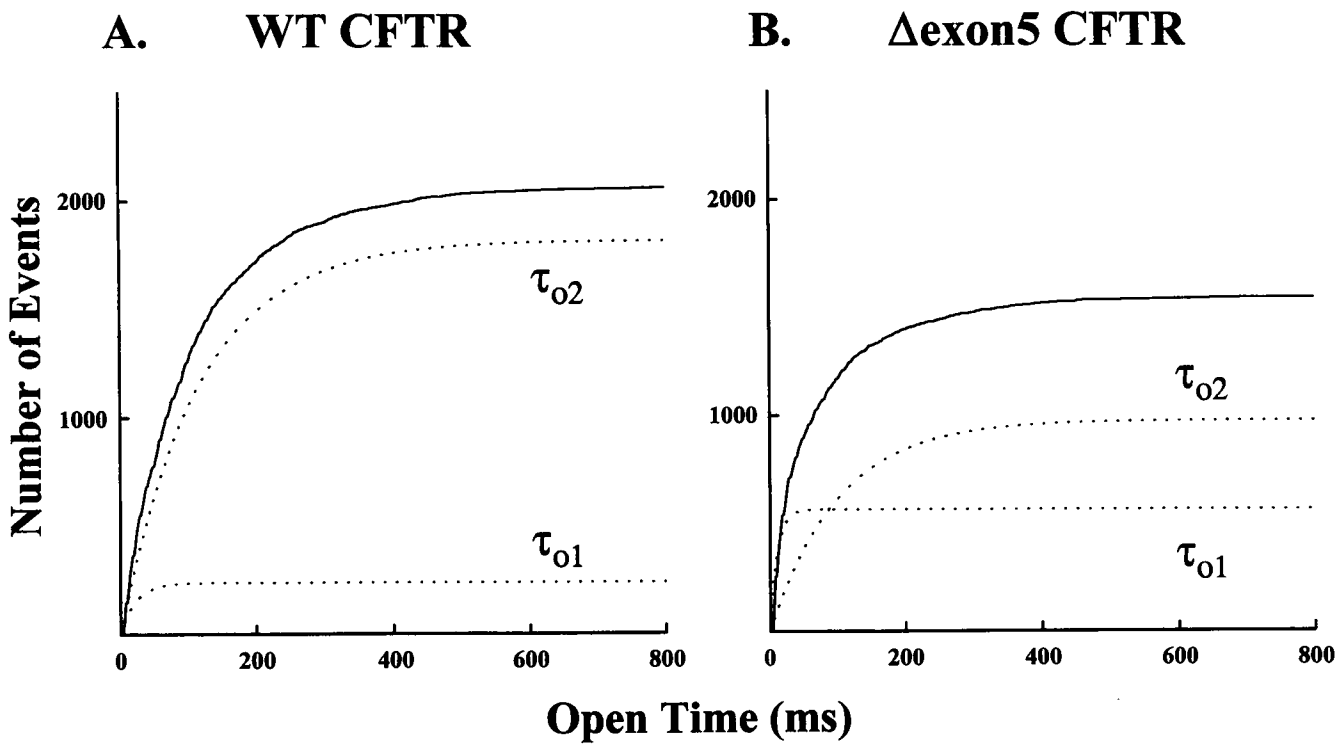

FIGURE 4 Channel kinetics of WT and Δexon5 CFTR channels. Open events were calculated at −80 mV, with WT (*A*) and Δexon5 (*B*) CFTR channels. A total of 208 episodes of 5-s test pulses to −80 mV was used for both (*A*) and (*B*). The number of events was 2062 for WT CFTR and 1494 for Δexon5 CFTR. The dotted curves labeled τ_{o1} and τ_{o2} represent the best fit according to the following equations: $y_1 = W_{o1}(1 - \exp(-t/\tau_{o1}))$ and $y_2 = W_{o2}(1 - \exp(-t/\tau_{o2}))$. The solid cuves represent $y = y_1 + y_2$, where W_{o1} = 237.26, W_{o2} = 1818.64, τ_{o1} = 22.31 ms, and τ_{o2} = 116.3 ms (*A*); and W_{o1} = 564.90, W_{o2} = 975.90, τ_{o1} = 10.60 ms, and τ_{o2} = 100.43 ms (*B*). All the open events were analyzed after 50-Hz digital filtering of single-channel currents recorded at 100-Hz cutoff filtering frequency.

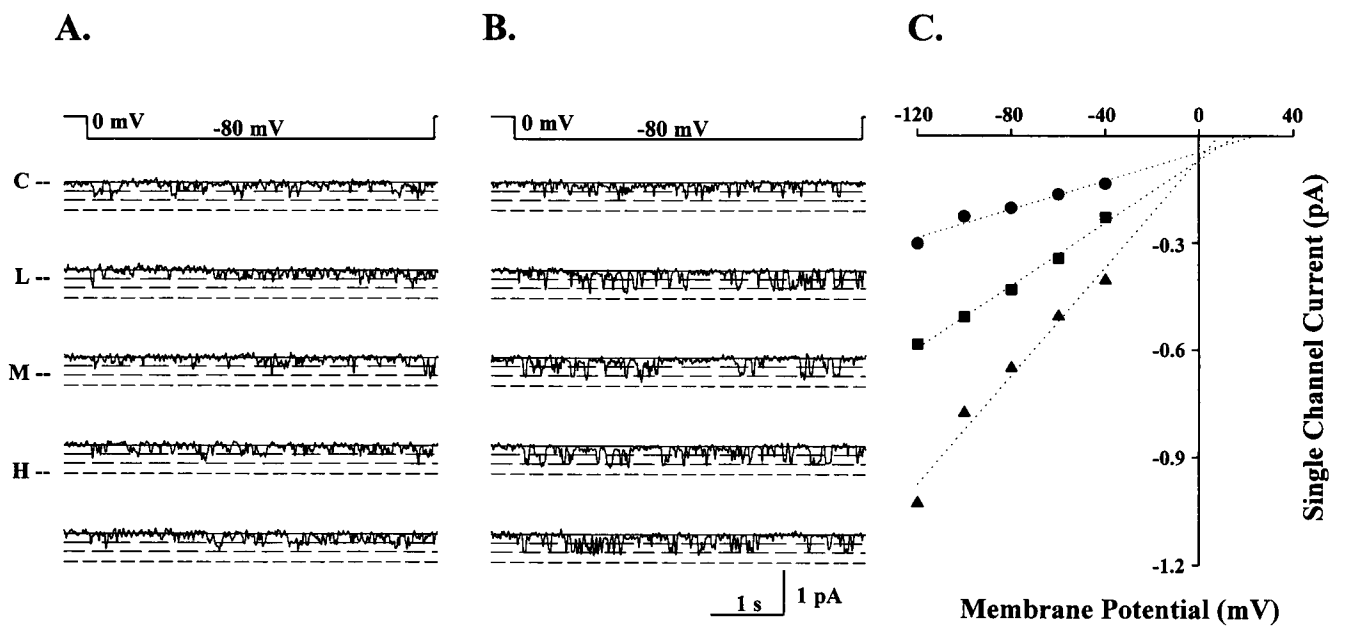

FIGURE 5 Subconductance states and current-voltage relationship of Δexon5 CFTR chloride channel. Consecutive single-channel current traces were plotted from two seperate experiments for Δexon5 CFTR channel. The bilayers were held at 0 mV, and the test potential was −80 mV. (*A*) The channel opens predominantly to the L subconductance state. (*B*) The channel opens stably to the M subconductance state. Dashed lines (*C, L, M, H*) are levels corresponding to closed, low, intermediate, and full conductance states, respectively. (*C*) Current–voltage relationship of the three conductance states of Δexon5 CFTR channel. ●, L subconductance state with a slope conductance of G = 2.0 ± 0.25 pS and extrapolated reversal potential (V_{rev}) of 23.3 ± 1.3 mV. ▲, Intermediate subconductance state with G = 4.4 ± 0.22 pS and V_{rev} = 15.4 ± 5.11 mV. ■, Full conductance state with G = 7.6 ± 0.76 pS and V_{rev} = 8.55 ± 9.30 mV. The dotted curves represent the best fit for the experimental data according to the least-squares criterion.

(Xie et al., 1995; Tao et al., 1996). Under conditions of 200 mM KCl (*cis*)/50 mM KCl (*trans*) with no extracellular divalent cations ($[Mg^{2+}]_o$ or $[Ca^{2+}]_o$), both the L and the H states could be measured in stable-single channel recordings, but rarely the M state (Table 1). Infrequently, transitions of H state to M state occurred in the WT CFTR channel but accounted for fewer than 10% of the open events (Xie et al., 1995). It is likely that the low (Fig. 5 *A*) and intermediate (Fig. 5 *B*) subconductance chloride channels of the Δexon5 CFTR correspond to the L and M subconductance states of the WT CFTR channel, as they share similar gating properties and pharmacological profiles. The average open probability estimated from the area under the amplitude histogram (Fig. 7 *A* and *B*) for the L subconductance state was 0.461 ± 0.194 for Δexon5 (n = 10) and 0.332 ± 0.142 for WT CFTR (n = 11). Although the P_o for Δexon5 appears to be higher than that of the WT CFTR (compare Fig. 7 *A* and *B*), they are not statistically significantly different (p = 0.073) from each other, probably because of the high variability from experiment to experiment and also the relatively high noise level compared with the low open amplitude of the L subconductance state. The conductance values for the three conductance states of Δexon5 CFTR were slightly lower than those of the WT CFTR (Fig. 5 *C*), possibly in part because of the heavy filtering frequency applied to the Δexon5 CFTR channel (30 Hz, instead of the 100 Hz used for the WT CFTR; Tao et al., 1996).

One significant difference between the WT and the Δexon5 CFTR was in the distribution of subconductance states. The low subconductance state of the WT CFTR occurred at low frequency (~17%), whereas for the Δexon5 CFTR channel the occurrence was more than 80% (Table 1). Therefore, deletion of exon 5 from the human epithelial CFTR caused the chloride channel to enter predominantly into the lower subconductance states.

A close examination of the single-channel traces revealed that the L subconductance state of the Δexon5 CFTR channel underwent frequent transitions to the M subconductance state when the extracellular solution did not contain $MgCl_2$ (Figs. 5 *A* and 7 *B*). The occurrence of the M subconductance state was greatly increased when 5 mM $MgCl_2$ was included in the extracellular solution (n = 8). The current amplitude histograms shown in Fig. 7 *B* and *C* were obtained from two separate experiments with the Δexon5 CFTR channel: in the absence of extracellular Mg^{2+} (Fig. 7 *B*) and in the presence of 5 mM extracellular Mg^{2+} (Fig. 7 *C*). Clearly, without extracellular Mg^{2+} the Δexon5 CFTR channel exhibits a dominant L subconductance state, and the addition of $[Mg^{2+}]_o$ resulted in the frequent transition to the M subconductance state. Similarly, in a continuous experiment the addition of divalent cations to the extracellular solution also caused conversion of Δexon5 CFTR channel open from the L state to the M state (n = 5; data not shown). This result indicates that extracellular Mg^{2+} could stabilize the M subconductance state of the Δexon5 CFTR channel.

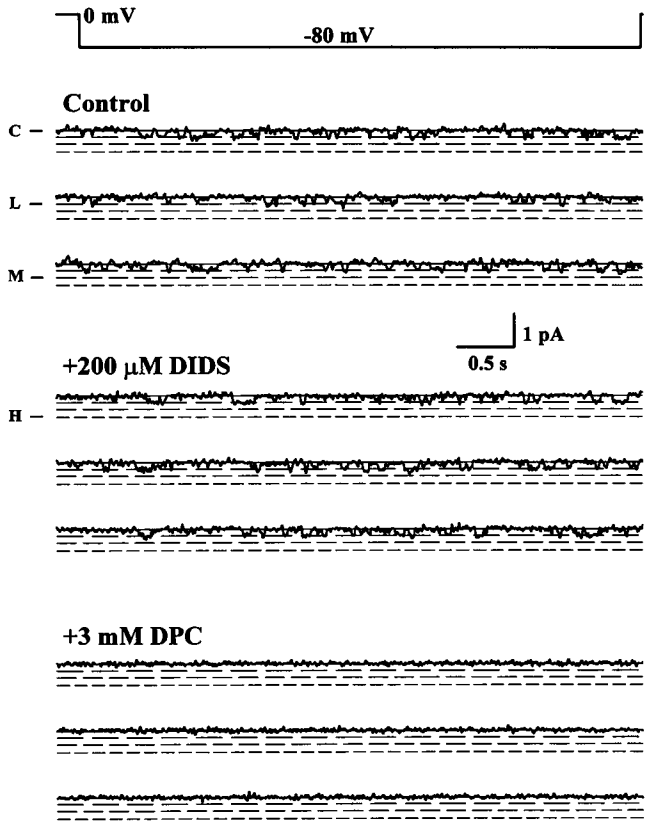

FIGURE 6 DPC and DIDS sensitivity of Δexon5 CFTR chloride channel. Consecutive single-channel current traces recorded at −80 mV test potential from a Δexon5 CFTR channel before (*Control*) and 2 min after addition of 3 mM DPC to the *trans*-extracellular solution. Single-channel current traces labeled +200 μM DIDS were consecutive channel records plotted for Δexon5 CFTR from a different experiment following application of DIDS for 10 min to the *trans*-extracellular solution. Data are representative of at least four other experiments. Dashed lines (*C, L, M, H*) are levels corresponding to closed, low, intermediate, and full conductance states, respectively. Not shown here are the data that both M and H conductance states are also sensitive to DPC blockade but not to DIDS (n = 3 each).

DISCUSSION

ΔExon5 CFTR is an alternatively spliced form of CFTR in guinea pig and rabbit heart membranes (Horowitz et al., 1993). This splicing variant is also found in mouse tissues but not in normal human epithelial cells (Delaney et al., 1993). In guinea pig and rabbit ventricular myocytes this isoform reportedly functions as a cAMP-regulated chloride channel with conduction properties similar to those of the human epithelial CFTR (Nagel et al., 1992; Overholt et al., 1995; Levesque et al., 1992). Recent studies (Hart et al., 1996) also showed that the expression CFTR cDNA isolated from rabbit ventricle in *Xenopus* oocytes gave rise to cAMP-regulated chloride current in the cell surface membrane. However, when expressed in HeLa cells, the human CFTR lacking exon 5 failed to generate a cAMP-mediated chloride transport across the cell plasma membrane measured by SPQ assay (Delaney et al., 1993). The apparent difference in processing between Δexon5 CFTR in human cells and that in guinea pig as well as in rabbit heart (Nagel et al., 1992; Overholt et al., 1995; Levesque et al., 1992) might be due to the differences between cardiac and epithelial cell systems or to the difference between the guinea pig and rabbit Δexon5 CFTR amino acid sequence compared with the human sequence, which might lead to slightly different structure and processing. Alternatively, rare WT CFTR transcripts could be present in guinea pig and rabbit heart cells, although all the detected CFTR transcripts were the alternatively spliced isoform in these species. It is not yet clear whether CFTR is also alternatively spliced in human heart. Levesque et al. (1992) detected CFTR message in human atrium. However, recent studies show that cAMP-stimulated chloride currents in human atrium are not carried through CFTR (Oz and Sorota, 1995; Li et al., 1996).

The present study shows that the human epithelial Δexon5 CFTR does not traffic to the plasma membrane of 293 HEK cells, which is consistent with the studies of Delaney et al. (1993) and Oz and Sorota (1995). The facts that a splice mutation that deletes exon 5 was found to be a cystic fibrosis disease-causing mutant and that there is an array of cystic fibrosis mutations in the region encoded by exon 5 (L165S, K166E, R170C, I175V, G178R, D192N, D192G, E193K; Fonknechten et al., 1992; Romey et al., 1994; Zielenski et al., 1991; Audrezet et al., 1994; Mercier et al., 1995; Cystic Fibrosis Mutation Data Base) suggest that exon 5 is important for the structure, function, or both of the CFTR chloride channel. Our data suggest that Δexon5 is a disease-causing CFTR mutant chiefly because it does not reach the plasma membrane. However, its channel function is abnormal as well.

Deleting the 30 amino acids encoded by exon 5 results in marked changes in its channel function and also in the distribution of subconductance states of the chloride channel compared with those for WT CFTR. The fact that we must study the Δexon5 CFTR protein function in intracellular membranes and WT CFTR in plasma membranes is unlikely to account for this difference. First, another intracellular loop deletion mutant, Δ19 CFTR, which also resides in intracellular membranes, shows functional similarity much closer to that of WT CFTR, although the occurrence of the M state is increased (Xie et al., 1995). In addition, the functional properties of ΔF508 and WT CFTR in the endoplasmic reticulum were reported to be similar to those measured in the cell surface membrane (Pasyk and Foskett, 1995). Moreover, the WT CFTR channel also opens stably to the L subconductance state in ~17% of the vesicle fusions and occasionally enters the M subconductance state. These observations suggest that the L and M subconductance states are likely intrinsic properties of CFTR protein but that the exon 5 deletion affects CFTR in such a way as to destabilize the H full conductance state but to favor the L and M subconductance states. Tao et al. (1996) found that extracellular Mg^{2+} stabilizes the H conductance state of the WT CFTR. However, extracellular Mg^{2+} did not increase the occurrence of the full H conduc

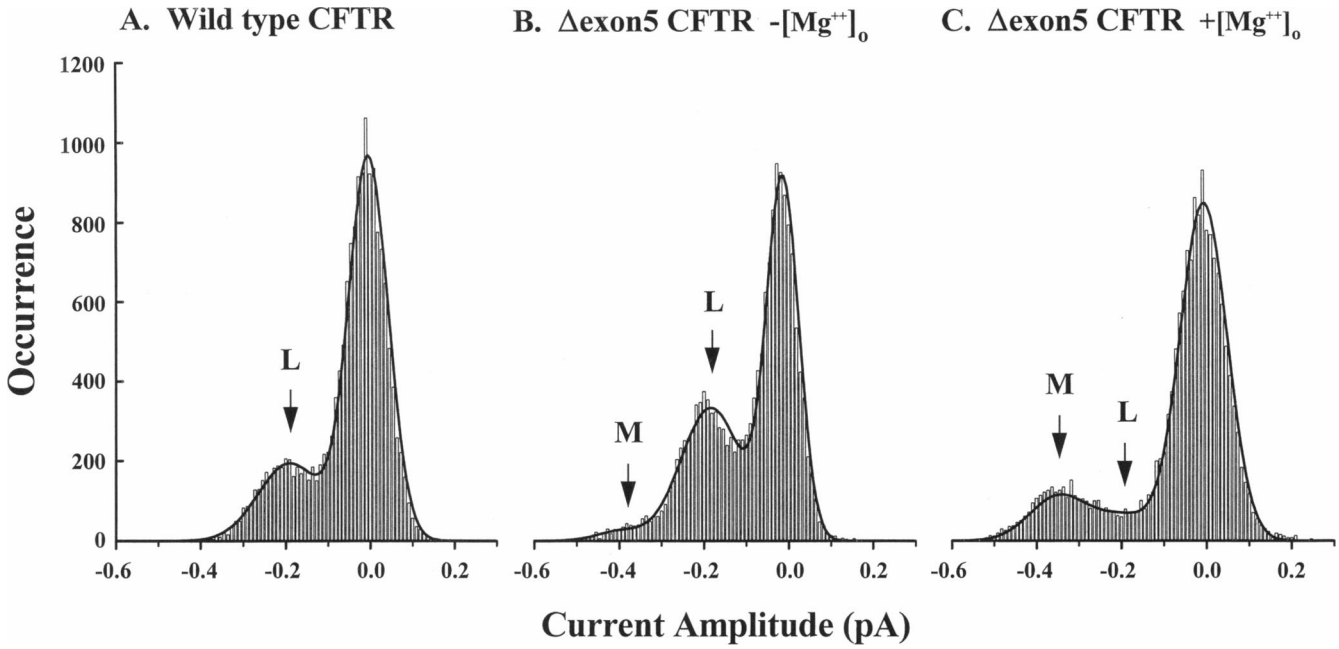

FIGURE 7 Effect of extracellular divalent cations on the conductance states of Δexon5 CFTR chloride channel. Channel current amplitude histograms representative of WT (*A*) and Δexon5 CFTR channels with (*C*) or without (*B*) extracellular $MgCl_2$ (5 mM). The solid curves represent the best fits with the sum of two (*A*) and three (*B* and *C*) Gaussian distribution functions: $y = W_1/(\sqrt{(2\pi)}\sigma_1)\exp[-(x - \mu_1)^2/(2\sigma_1^2)] + W_2/(\sqrt{(2\pi)}\sigma_2)\exp[-(x - \mu_2)^2/(2\sigma_2^2)] + W_3/(\sqrt{(2\pi)}\sigma_3)\exp[-(x - \mu_3)^2/(2\sigma_3^2)]$, where $W_1 = 113.02$, $\mu_1 = -0.004$ pA, $\sigma_1 = 0.047$ pA, $W_2 = 36.38$, $\mu_2 = -0.191$ pA, $\sigma_2 = 0.075$ pA (*A*); $W_1 = 87.08$, $\mu_1 = -0.014$ pA, $\sigma_1 = 0.039$ pA, $W_2 = 57.65$, $\mu_2 = -0.186$ pA, $\sigma_2 = 0.068$ pA, $W_3 = 3.46$, $\mu_3 = -0.387$ pA, $\sigma_3 = 0.042$ pA (*B*); and $W_1 = 116.52$, $\mu_1 = -0.007$ pA, $\sigma_1 = 0.055$ pA; $W_2 = 10.10$, $\mu_2 = -0.189$ pA, $\sigma_2 = 0.068$ pA; $W_3 = 21.64$, $\mu_3 = -0.348$ pA, $\sigma_3 = 0.068$ pA (*C*). (*L* ↓) Low open level, (*M* ↓) intermediate open level. Channel current in (*A*) was recorded at 100-Hz cutoff frequency; those in (*B*) and (*C*) were recorded at 30-Hz cutoff frequency. All the data were subjected to 30-Hz digital filtering before analysis.

tance state for Δexon5 CFTR; instead it stabilized the M subconductance state. The exact mechanisms of how extracellular divalent cations are involved in stabilizing the full conductance state of the WT CFTR chloride channel and the intermediate conductance state of the Δexon5 CFTR chloride channel remain to be investigated further.

Several factors could account for the abnormal single-channel function and the predominant subconductance states associated with the Δexon5 CFTR channel. One possibility is that the first intracellular loop participates in intermolecular interactions between CFTR molecules. If different subconductance states within CFTR arise from different aggregation states of multiple CFTR molecules (Tao et al., 1996), a deletion in the first intracellular loop could disrupt these intermolecular interactions, thus altering the distribution of subconductance states associated with CFTR chloride channel. Although some lines of evidence suggest that CFTR functions as a monomer (Marshall et al., 1994), the exact stoichiometry of a functional CFTR channel, i.e., whether the full conductance state of the CFTR represents a single 170-kDa CFTR polypeptide or a multimer, remains uncertain.

A second possibility is that the altered channel behavior of Δexon5 results from intramolecular interactions within CFTR, for example, between the first intracellular loop and other cytosolic domains (R, NBDs, or other intracellular loops). The altered single-channel kinetics in the full conductance state (e.g., the less frequent occurrence of the longer open events as well as the total channel events) suggests possible interactions of the first intracellular loop with the NBDs (Carson et al., 1995). It is also possible that the positively charged first intracellular loop (+7) could interact electrostatically with the negatively charged R domain on phosphorylation to confer different open states. The deletion mutation in the first intracellular loop may destabilize or disrupt those electrostatic interactions when the phosphorylated channel assumes its full open configuration.

Another possibility is that the first intracellular loop simply contributes to the overall structure of CFTR channel sterically and that shortening this loop has an allosteric effect on CFTR structure to destabilize the full conductance configuration. Consistent with this hypothesis are the studies of Carroll et al. (1995), in which deletion mutations (Δ119, Δ256) that removed transmembrane segment I or transmembrane segments I-IV caused reductions in both single-channel conductance and open probability of CFTR chloride channel. To test this hypothesis further it will be necessary to study whether deletions from other parts of the first intracellular loop or substitutions also affect the function of the CFTR chloride channel.

In summary, our present studies show that exon 5 is important for processing as well as for function of the CFTR chloride channel. Further investigations into the function of CF disease-causing mutations in the region encoded by exon 5 may

provide us more information about the role(s) of the first intracellular loop in CFTR chloride channel function.

We thank Dr. Harvey B. Pollard for helpful discussions on channel subconductance states. This research was supported by a Research Development Program grant from the Cystic Fibrosis Foundation by and grants from the National Institutes of Health (P30 DK27651 and RO1HL/DK49003).

REFERENCES

Anderson, M. P., H. A. Berger, D. P. Rich, R. J. Gregory, A. E. Smith, and M. J. Welsh. 1991b. Nucleoside triphosphates are required to open the CFTR chloride channel. *Cell.* 67:775–784.

Anderson, M. P., R. J. Gregory, S. Thompson, D. W. Souza, S. Paul, R. C. Mulligan, A. E. Smith, and M. J. Welsh. 1991a. Demonstration that CFTR is a chloride channel by alteration of its anion selectivity. *Science.* 253:202–207.

Audrezet, M. P., K. N. Canki, B. Mercier, M. Bracar, C. Verlingue, and C. Ferec. 1994. Identification of three novel mutations (457 TAT → G, D192G, Q685X) in the Slovenian CF patients. *Hum. Genet.* 93:659–662.

Baukrowitz, T., T.-C. Hwang, A. C. Nairn, and D. C. Gadsby. 1994. Coupling of CFTR Cl^- channel gating to an ATP hydrolysis cycle. *Neuron.* 12:473–482.

Bear, C. E., C. Li, N. Kartner, R. J. Bridges, T. J. Jensen, M. Ramjeesingh, and J. R. Riordan. 1992. Purification and functional reconstitution of the cystic fibrosis transmembrane conductance regulator (CFTR). *Cell.* 68: 809–818.

Carroll, T. P., M. M. Morales, S. B. Fulmer, and S. S. Allen. 1995. Alternate translation initiation codons can create functional forms of cystic fibrosis transmembrane conductance regulator. *J. Biol. Chem.* 270:11,941–11,946.

Carson, M. R., S. M. Travis, and M. J. Welsh. 1995. The two nucleotide-binding domains of cystic fibrosis transmembrane conductance regulator (CFTR) have distinct functions in controlling channel activity. *J. Biol. Chem.* 270:1711–1717.

Chang, X.-B., J. A. Tabcharani, Y.-X. Hou, T. J. Jensen, N. Kartner, N. Alon, J. W. Hanrahan, and J. R. Riordan. 1993. Protein kinase A (PKA) still activates CFTR chloride channel after mutagenesis of all 10 PKA consensus phosphorylation sites. *J. Biol. Chem.* 268:11,304–11,311.

Cheng, S. H., D. P. Rich, J. Marshall, R. J. Gregory, M. J. Welsh, and A. E. Smith. 1991. Phosphorylation of the R domain by cAMP-dependent protein kinase regulates the CFTR chloride channel. *Cell.* 66:1027–1036.

Cystic Fibrosis Mutation Data Base. Http://www.genet.sickkids.on.ca/cftr/: *NL* #51, #62, #66, #67.

Delaney, S. J., D. P. Rich, S. A. Thompson, M. R. Hargrave, P. K. Lovelock, M. J. Welsh, and B. J. Wainwright. 1993. Cystic fibrosis transmembrane conductance regulator splice variants are not conserved and fail to produce chloride channels. *Nature Genet.* 4:426–431.

Denning, G. M., M. P. Anderson, J. F. Amara, J. Marshall, A. E. Smith, and M. J. Welsh. 1992. Processing of mutant cystic fibrosis transmembrane conductance regulator is temperature-sensitive. *Nature (London).* 358: 761–764.

Drumm, M. L., D. J. Wilkinson, L. S. Smit, R. T. Worrell, T. V. Strong, R. A. Frizzell, D. C. Dawson, and F. S. Collins. 1991. Chloride conductance expressed by ΔF508 and other mutant CFTRs in *Xenopus* oocytes. *Science.* 254:1797–1799.

Fonknechten, N., J.-C. Chomel, A. Kitzis, A. Kahn, and J.-C. Kaplan. 1992. Skipping of exon 5 as a consequence of the 711+IG→T mutation in CFTR gene. *Hum. Mol. Genet.* 1:281–282.

Hart, P., J. D. Warth, P. C. Levesque, M. L. Collier, Y. Geary, B. Horowitz, and J. R. Hume. 1996. Cystic fibrosis gene encodes a cAMP-dependent chloride channel in heart. *Proc. Natl. Acad. Sci. USA.* 93:6343–6348.

Hawley-Nelson, P., V. Ciccarone, G. Gebeyehu, J. Jessee, and P. L. Felgner. 1993. LipofectAMINE™ reagent: a new, higher efficiency polycationic liposome transfection reagent. *Focus.* 15:73–79.

Horowitz, B., S. S. Tsung, P. L. Hart, P. C. Levesque, and J. R. Hume. 1993. Alternative splicing of CFTR Cl^- channels in heart. *Am. J. Physiol.* 264:H2214–H2220.

Levesque, P. C., P. J. Hart, J. R. Hume, J. L. Kenyon, and B. Horowitz. 1992. Expression of cystic fibrosis transmembrane regulator Cl^- channels in heart. *Circ. Res.* 71:1002–1007.

Li, G., J. Feng, Z. Wang, and S. Nattel. 1996. Transmembrane chloride currents in human atrial myocytes. *Am. J. Physiol.* 270:C500-C507.

Lukacs, G. L., X.-B. Chang, C. Bear, N. Kartner, A. Mohamed, J. R. Riordan, and S. Grinstein. 1993. The ΔF508 mutation decreases the stability of cystic fibrosis transmembrane conductance regulator in the plasma membrane. Determination of functional half-lives on transfected cells. *J. Biol. Chem.* 268:21,592–21,598.

Ma, J., J. E. Tasch, T. Tao, J. Zhao, J. Xie, M. L. Drumm, and P. B. Davis. 1996. Phosphorylation-dependent block of cystic fibrosis transmembrane conductance regulator chloride channel by exogenous R domain protein. *J. Biol. Chem.* 271:7351–7356.

Marshall, J., S. Fang, L. S. Ostedgaard, C. R. O'Riordan, D. Ferrara, J. F. Amara, H. IV. Hoppe, R. K. Scheule, M. J. Welsh, A. E. Smith, and S. H. Cheng. 1994. Stoichiometry of recombinant cystic fibrosis transmembrane conductance regulator in epithelial cells and its functional reconstitution into cells in vitro. *J. Biol. Chem.* 269:2987–2995.

Mercier, B., C. Verlingue, W. Lissens, S. J. Silber, G. Novelli, M. Bondnelle, M. P. Audrezet, and C. Ferec. 1995. Is congenital bilateral absence of vas deferens a primary form of cystic fibrosis? Analyses of the CFTR gene in 67 patients. *Am. J. Genet.* 56:272–277.

Nagel, G., T. C. Hwang, K. L. Nastiuk, A. C. Nairn, and D. C. Gadsby. 1992. The protein kinase A–regulated cardiac Cl^- channel resembles the cystic fibrosis transmembrane conductance regulator. *Nature (Lond.).* 360:81–84.

Overholt, J. L., A. Saulino, M. L. Drumm, and R. D. Harvey. 1995. Rectification of whole cell cystic fibrosis transmembrane conductance regulator chloride current. *Am. J. Physiol.* 268:C636-C646.

Oz, M. C., and S. Sorota. 1995. Forskolin stimulates swelling-induced chloride current, not cardiac cystic fibrosis transmembrane-conductance regulator current, in human cardiac myocytes. *Circ. Res.* 76:1063–1070.

Pasyk, E. A., and J. K. Foskett. 1995. Mutant (ΔF508) cystic fibrisis transmembrane conductance regulator chloride channel is functional when retained in endoplasmic reticulum of mammalian cells. *J. Biol. Chem.* 270:12,347–12,350.

Pind, S., A. Mohamed, X.-B. Chang, Y.-X. Hou, T. J. Jensen, D. B. Williams, and J. R. Riordan. 1995. Multiple initiation sites are used during translation of the mRNA encoding CFTR. *Pediatr. Pulmonol.* 12:180.

Quinton, P. M., and M. M. Reddy. 1992. Control of CFTR chloride conductance by ATP levels through non-hydrolytic binding. *Nature (London).* 360:79–81.

Rich, D. P., H. A. Berger, S. H. Cheng, S. M. Travis, M. Saxena, A. E. Smith, and M. J. Welsh. 1993. Regulation of the cystic fibrosis transmembrane conductance regulator chloride channel by negative charge in the R domain. *J. Biol. Chem.* 268:20,259–20,267.

Riordan, J. R., J. M. Rommens, B.-S. Kerem, N. Alon, R. Rozmahel, Z. Grzelczak, J. Zielenski, S. Lok, N. Plavsic, J.-L. Chou, M. L. Drumm, M. C. Iannuzzi, F. S. Collins, and L. C. Tsui. 1989. Identification of the cystic fibrosis gene: cloning and characterization of complementary DNA. *Science.* 245:1066–1073.

Romey, M. C., M. Desgeorges, P. Malzac, J. Sarles, J. Demaille, and M. Claustres. 1994. Homozygosity for a novel missense mutation (I175V) in exon 5 of the CFTR gene in a family of Armenian descent. *Hum. Mol. Genet.* 3:661–662.

Tao, T., J. Xie, M. L. Drumm, J. Zhao, P. B. Davis, and J. Ma. 1996. Slow conversions among sub-conductance states of cystic fibrosis conductance regulator chloride channel. *Biophys. J.* 70:743–753.

Xie, J., M. L. Drumm, J. Ma, and P. B. Davis. 1995. Intracellular loop between transmembrane segments IV and V of cystic fibrosis conductance regulator is involved in regulation of chloride channel conductance state. *J. Biol. Chem.* 270:28,084–28,091.

Zielenski, J., D. Bozon, B. S. Kerem, D. Markiewicz, P. Durie, J. M. Rommens, and L. C. Tsui. 1991. Identification of mutations in exons 1 through 8 of the cystic fibrosis transmembrane conductance regulator (CFTR) gene. *Genomics.* 10:229–235.